Robust and Randomized Control Design of Mini-UAVs: The MH1000 Platform

L. Lorefice*, B. Pralio* and R. Tempo**
* Politecnico di Torino/Dipartimento di Ingegneria Aeronautica e Spaziale, Torino, Italy
** IEIIT-CNR, Torino, Italy

Abstract— **Mini-UAVs (Unmanned Aerial Vehicles) have been the subject of a large number of successful designs aimed to research, commercial and military purposes. A mini-UAV platform can be considered as a miniaturized aircraft so that classical design methodologies can be extended to this aerial vehicles category. However, due the presence of plant uncertainties, flight dynamic analysis and control system design are critical, and suitable robustness techniques need to be developed. In this paper, we present an innovative robust control strategy based on powerful tools provided by the theory of randomized algorithms. Within the context of the National Project Cofin 2004, the proposed methodology has been implemented for guidance/trajectory tracking and platform stabilization feedback loops of the autopilot system. The numerical results obtained are presented.**

I. INTRODUCTION

Unmanned Aerial Vehicles (UAVs) have become increasingly attractive for industries as well as for researchers in aeronautics for various economic and safety reasons. These platforms can be remotely controlled or they can autonomously fly without pilot on-board, for surveillance and reconnaissance missions in dangerous areas. Clearly, they encounter a great number of useful applications both in civil and military fields. Among the military applications, surveillance, targeting and communications can be counted. Civil missions also have several objectives, which in some cases coincide with military ones. In particular, UAV platforms enable localization of missing people, reconnaissance and surveillance of territories such as steep slopes, traffic monitoring, fire and rescue operations, biochemical sensing and sensor placement. These platforms can be divided into different categories according to size, endurance or mission range, but one of the most common classifications of UAV typologies available in the literature is related to the platform size.

In the last decade, the acronym MAVs (Micro Aerial Vehicles) has been used to define flying objects characterized by physical size approximately smaller than 6 inches, in length, width or height. Recalling a classical definition [1], these flying objects can be considered as ``aerial robots, as six-degree-of freedom machines whose mobility can deploy a useful micropayload to a remote, or otherwise hazardous location, where it may perform any of a variety of missions." The concept of uninhabited aerial vehicles of reduced dimensions, able to perform mission profiles not compatible with any existing piloted platforms, was subsequently extended to bigger systems and it now incorporates the so-called Mini-UAVs, having maximum dimension up to 6 ft. These platforms have been the subject of considerable interest and development in recent years. A large number of successful designs have been performed for either research, commercial or military purposes by several universities, industries and government-funded agencies both in the US as well as in Europe.

As a consequence of different applications and, hence, a different range-payload performance, several configuration concepts can be encountered within the Mini-UAV category. In fact, a fixed wing Mini-UAV can be considered as a miniaturized aircraft so that preliminary design issues and procedures applied to conventional platforms can be extended to this family of aerial vehicles. In spite of that, aircraft dynamics and flight control system definitions represent critical issues, influencing the approach for the design and flight testing phases. The reduced dimensions of these vehicles lead to highly nonlinear system behavior and unconventional dynamics in terms of natural frequencies and damping ratios. The inertial characteristics of the platform yield to unconventional mode characterization thus resulting in undesirable abrupt responses to piloted commands. Furthermore, the sensitivity to changes in flight conditions (concerning velocity more than altitude), the assumptions in aerodynamic database definition (e.g., stability and control derivatives), the inaccuracies in geometric and inertial data represent a set of uncertainties in plant and environment modeling. The result is that conventional control design methods are often not effective [2]. Therefore, the design of a flight control system which guarantees a suitable level of tolerance to environmental changes and platform manufacturing/modelling inaccuracies plays a key role whenever stability and performance requirements have to be fulfilled, see e.g. [3].

Micro and Mini-UAVs represent a major challenge for control design, and robust control in particular. Robust control algorithms may be viewed as complementary to gain scheduling and fault tolerant control methods. In fact, the problem of searching the appropriate gains can be reformulated in terms of operating conditions representing the critical parameters by means of dynamic pressure and/or Mach number. On the other hand, the use of a fault tolerant approach strongly depends on the failure effects modeling. The failure types to be dealt with by the proposed methodology are related to finding an explicit

relationship between the failure entity and the plant parameters. Whenever this relationship is available, the critical parameters leading to instability or loss of performance may be easily detected.

The applicability of various classical robustness techniques such as, for example, Linear Matrix Inequalities and related relaxation methods, and μ-theory [4], has been explored for the MH1000 platform. However, the mathematical model is affected by nonlinear uncertainty of parametric type. In addition, this model is obtained by numerical linearization of the full order nonlinear system representing the aircraft dynamics, so that explicit relationships between the state-space matrices and the uncertain parameters are not available. For these reasons, in this paper we follow a different innovative approach for gain synthesis. This approach makes use of uncertainty randomization and is based on the theory of *randomized algorithms* [5]. These algorithms are easy to implement, have low computational complexity and are associated with robustness bounds that are generally less conservative than the classical ones, obviously at the expense of a probabilistic risk of failure.

The theory of randomized algorithms follows the pioneering line of research that was initiated by Stengel [6] in the early eighties. In several subsequent papers [7][8][9] and references therein, various techniques, mainly based on Monte Carlo simulations, have been explored for the computation of the probability of instability, and related performance concepts. The application area providing motivations for the development of these methods is indeed aerospace control, and the results obtained are very successful. In this line of research, specific attention is devoted to reduced order models of the aircraft dynamics by analyzing the effects of aerodynamic uncertainties.

We now describe the organization of the paper and the main results obtained. In Section II, we briefly introduce the MH1000 platform, representing the reference platform for the control algorithms testing. In Section III, we present the mathematical formulation of the plant dynamics. This formulation is based upon a full six degrees-of-freedom nonlinear mathematical model, see [10] for details. Uncertainty characterization is the focus of Section IV. We consider the vector of ℓ real uncertain parameters δ_i, restricted within upper and lower bounds. In addition, each parameter δ_i is a random variable with an assigned probability density function, either uniform or truncated normal, within this interval. Uncertainties for the MH1000 platform include parameters related to flight conditions, aerodynamic data, geometric and inertial data, see Section IV for a precise description. In this section, we also briefly introduce the concept of *specification property* S which is utilized subsequently in the randomized algorithms. In Section V, we present three randomized algorithms which should be used sequentially. The first algorithm is based upon the selection of a subset of *m* critical uncertain parameters, and has the objective to provide an initial set of randomly generated controller gains K_{rand}. The specification property is explicitly defined and a stopping criterion in terms of the probabilistic *confidence* and *accuracy* is given. This stopping criterion is based upon the so-called "Log-over-log" Bound [11]. Algorithm 2 uses a set of gains K_{rand} previously obtained and computes the empirical probability that given performance specifications are satisfied. To this end, a bound on the required sample size, the Chernoff Bound [12] is utilized. Finally, Algorithm 3 has a structure similar to Algorithm 2, but different specification properties, derived from standard flying qualities of piloted aircraft [13], are used. In Section VI we present the numerical results related to the case study. In particular, in this section, classical graphical tools, such as the root locus plot and the standard bandwidth levels, highlighting the region of interest defined by the specification property, are used to compare various solutions and to single out the best fitting one. The conclusions are given in Section VII.

II THE MH1000 PLATFORM

The aerial platform MH1000 is based on the MicroHawk configuration, developed at the Aerospace Engineering Department, Politecnico di Torino (national patent no. TO2003A000702, holder Politecnico di Torino, international request PCT/IB2004/002940). The reference platform is characterized by a conventional layout consisting of fixed wing, tailless integrated wing-body configuration, tractor propeller driven. A scaled version of the MicroHawk configuration, named MH1000 (Fig. 1), characterized by 1 m wingspan and a total weight of approximately 1.5 kg, was designed and tuned to meet the mission specifications required by the project. The flight envelope of the platform ranges from 40 kph to 72 kph; an average flight speed of about 55 kph allows to achieve a flight endurance of at least 40 minutes. The platform flight performances, the autopilot system effectiveness and the compliance of the integrated system to the mission requirements have been tested by extensive on-site flight tests, also in cooperation with the Environment Protection and Damage Preemption Agency of Sicily.

Fig. 1: The MH1000 platform during a flight test.

III PLANT DYNAMICS

The aerial platform is described by a full six degrees-of-freedom nonlinear mathematical model, consisting of twelve, coupled, nonlinear, ordinary differential equations [10]. The model is based on three point mass equations, three attitude dynamics equations, three kinematical relationships and three navigation equations for trajectory evaluation. The equations of motion, both for point mass center of gravity dynamics and for attitude dynamics, are written with reference to the body-axes reference frame, i.e. a vehicle body-fixed system, having origin at the vehicle center of gravity and axes aligned to vehicle reference directions. Structural flexibility is neglected so that the rigid body assumption is made. This assumption is commonly used in general flight simulations since the

attention is focused on trajectory analysis and overall aircraft performance. Furthermore, this assumption makes sense because we are dealing with a Mini-UAV characterized by small dimensions and weight. The flat and non-rotating Earth assumption is also used since it does not affect model accuracy of low speed flight over a small region of the Earth. Finally, the aerodynamic loads acting on the aerial platform are obtained utilizing an aerodynamic model, based on experimental wind tunnel testing and numerical computations.

The point mass center of gravity dynamics and the attitude dynamics equations, written in matrix notation, are given by:

$$\{\dot{V}_E\}_B = \frac{1}{m}\{F_{A,T}\}_B - [\Omega_{\omega_B}]_B\{V_E\}_B - [T_{VB}]^{-1}\{g\}_V$$
$$\{\dot{\omega}_B\} = [I]_B^{-1}\left\{\{M_{A,T}\} - [\Omega_{\omega_B}]_B([I]_B\{\omega\}_B)\right\}$$

where the body-axes components of the velocity vector $\{V_E\}_B$ and of the angular velocity vector $\{\omega\}_B$ are

$$\{V_E\}_B = [U\ V\ W]^T$$
$$\{\omega\}_B = [P\ Q\ R]^T$$

The aerodynamic and propulsive forces and moments vectors are represented by the vectors $\{F_{A,T}\}_B$ and $\{M_{A,T}\}_B$, respectively. The matrix $[I]_B$ and m are the inertia matrix and the mass of the rigid body, respectively, and $[\Omega_{\omega B}]_B$ is the cross-product matrix of the angular velocity vector $\{\omega\}_B$. Finally, $\{g\}_V$ is the gravity acceleration expressed in the local navigation reference (NED axis) system and the matrix $[T_{VB}]$ represents the rotation matrix from body to NED reference system.

The vehicle attitude is modeled by the Euler kinematical equations:

$$\{\dot{\Phi}\} = [T_{VA}]\{\omega\}_B$$

where the Euler angles vector $\{\Phi\}=\{\phi\ \theta\ \psi\}$ consists of roll, pitch and yaw, respectively. The matrix $[T_{VA}]$ denotes the kinematical relationship between the Euler angles and the angular velocities.

The navigation equations for trajectory evaluation is expressed by

$$\{\dot{p}\} = [T_{VB}]\{V_E\}_B$$

where the vector $\{p\}=\{X_V\ Y_V\ Z_V\}$ represents the center of gravity coordinates in a geographic system having origin at the vehicle center of gravity.

The mathematical formulation also includes the modelling of the main subsystems (engine, propeller, actuators). As to the propulsive system, linear relationships are applied to model the voltage supply and current drain trend of variation for a DC motor-based propulsion. The propeller performance is estimated by implementing the blade element theory to compute propulsive forces and moments at a given regime of rotation [14].

A state-space formulation is obtained by numerical linearization of the full order system around an equilibrium condition ($\dot{x}_0$, x_0, u_0). The numerical linearization algorithm is based on the implicit formulation of the ordinary differential equations representing the aircraft dynamics:

$$h(\dot{x}, x, u) = 0$$

where x represents the vector of state variables and u is the vector of control variables.

IV UNCERTAINTY CHARACTERIZATION

To characterize parametric uncertainty, the standard state-space formulation is used to re-write the linearized system of the plant dynamics:

$$\dot{x}(t) = A(\Delta)x(t) + B(\Delta)u(t)$$

where $A \in \mathbf{R}^{n,n}$, $B \in \mathbf{R}^{n,p}$, and Δ consists of ℓ uncertain parameters, i.e.,

$$\Delta = [\delta_1, \delta_2, \cdots, \delta_\ell]^T$$

The controller structure we use is a state-feedback of the form $u = -K x$, so that the problem is to find a gain matrix K satisfying given specifications

$$K = \begin{bmatrix} k_{11} & k_{12} & \cdots & k_{1n} \\ k_{21} & k_{22} & \cdots & k_{2n} \\ \vdots & \vdots & \ddots & \vdots \\ k_{p1} & k_{p2} & \cdots & k_{pn} \end{bmatrix}$$

Next, we assume that each uncertain parameter δ_i is a random variable distributed according to a given probability density function (p.d.f.) $p_{\delta i}(\delta_i)$, in the interval $[\delta_i^-, \delta_i^+]$. We define the set

$$\mathcal{B}_\Delta = \{\Delta : \delta_i \in [\delta_i^-, \delta_i^+],\ i = 1, 2, \ldots, \ell\}$$

In particular, the parameter δ_i may be uniformly distributed or distributed according to a truncated Gaussian density. Then, we consider N_Δ independent identically distributed (i.i.d.) samples

$$\Delta^j = [\delta_1^j, \delta_2^j, \cdots, \delta_\ell^j]^T$$

of the random vector Δ. In particular, this means that the sample δ_i^j of the random parameter δ_i is drawn within the interval $[\delta_i^-, \delta_i^+]$ according to the distribution $p_{\delta i}(\delta_i)$.

The next step is to introduce a suitable *specification property* S, which is the set of all controller gains or uncertain parameters satisfying suitably defined closed loop specifications. In particular, S_1 refers to controller gains K, while S_2 and S_3 are related to uncertain parameters. Concrete instances of specification properties for the MH1000 platform are provided in Section VI and include, for example, limits on the step or frequency response, or restrict the natural frequency and damping ratio to a given range.

In the first (synthesis) phase, we also assume that the gain matrix K is random. Then, we take N_K i.i.d. matrix samples

$$\{K^1, K^2, \ldots, K^{NK}\}.$$

In particular, the sample k^j_{im} of the random gain k_{im} is drawn within the given interval $[k^-_{im}, k^+_{im}]$ according to a uniform distribution. We define the set

$$\mathcal{B}_K = \{K : k_{im} \in [k^-_{im}, k^+_{im}], i = 1, 2, \ldots, p, m = 1, 2, \ldots, n\}$$

The objective is to find a gain matrix $K_{rand} = K^j$ which satisfies the specification property S_1. Clearly, it is important to determine the sample size N_K which provides a stopping rule in the randomized algorithms described later in Section V. To this end, we use an explicit bound often denoted "Log-over-log" which is based on two probabilistic quantities, restricted within the intervals (0,1), denoted as *accuracy* ε and *confidence* η, see [11] and [5] for details.

Let $\{K^1, K^2, \ldots, K^s\}$ be the random matrices satisfying S_1, where s denotes the number of *successes*, i.e., the number of matrix gains satisfying S_1. The second (robustness) phase utilizes $K_{rand}=K^j$, j=1,2, …,s, previously computed and has the objective to estimate the "true" probability p_{true} that the specification property S_2 is satisfied. Formally, we define

$$p_{true} = \int_{\{\Delta \in B_\Delta \cap S_2\}} p(\Delta) d\Delta$$

Then, we introduce the indicator function

$$I(\Delta^j) = \begin{cases} 1 & \text{if } \Delta^j \in S_2 \\ 0 & \text{otherwise} \end{cases}$$

The estimated probability that the specification property S_2 is satisfied is immediately given by

$$\hat{p}_{N_\Delta} = \frac{1}{N_\Delta} \sum_{j=1}^{N_\Delta} I(\Delta^j)$$

The estimate $p_{N\Delta}$ is usually referred to as *empirical probability*. The sample size needed to obtain a "reliable probabilistic estimate" $p_{N\Delta}$ is given by the Chernoff Bound, see [12] and [5] for further discussions on this topic.

V RANDOMIZED ALGORITHMS FOR GAIN SYNTHESIS AND ROBUSTNESS ANALYSIS

Three randomized algorithms for gain synthesis and robustness analysis are shown in this section. As previously discussed, the controller structure is a state-feedback of the form $u = -K x$, so that the problem is to find a suitable gain matrix K. Three algorithms are presented for gain synthesis, stability analysis and performance analysis, respectively. The algorithms are strongly coupled and closely related to the operating flight conditions and to the flying quality standards. In particular, the algorithms are used sequentially: Algorithm 1 is used for synthesis to provide an initial set of controller gains, while Algorithms 2 and 3 are then used to improve robustness. The performance requirements specified in Algorithm 3 are different than those of Algorithm 2, so that refinements on the choice of gains are provided.

Algorithm 1 (Fig. 2) is based upon the selection of a subset of $m \le \ell$ *critical* uncertain parameters. That is, we consider a vector Δ_c containing only m components of Δ:

$$\Delta_c = [\delta_1, \delta_2, \cdots, \delta_m]^T$$

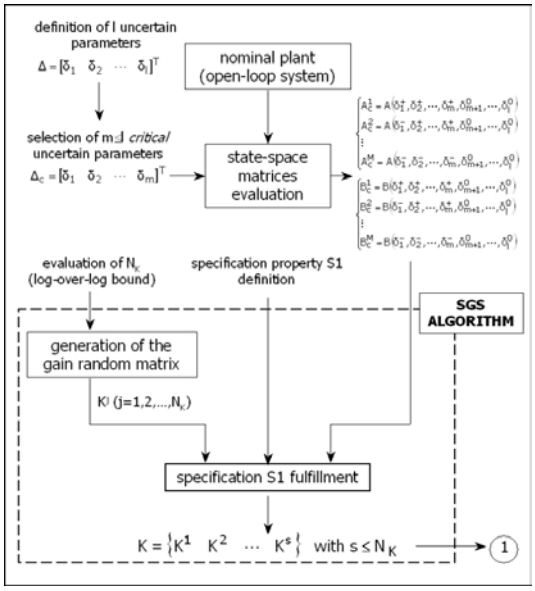

Fig. 2: Algorithm 1 – Random Gain Selection.

Then, setting the critical uncertain parameters to all combinations of their upper or lower values δ_i^+ or δ_i^-, suitable controller gains are randomly selected. This selection makes use of a given p.d.f. of controller gains and their a priori bounds. The remaining non-critical parameters are set to their corresponding nominal value, i.e., δ_i^0, $i = m+1, \ldots, \ell$. Clearly, since the state-space matrices $A(\Delta)$ and $B(\Delta)$ depend on Δ, this requires to compute $M = 2^m$ critical matrices of the form:

$$\begin{cases} A_c^1 = A(\delta_1^+, \delta_2^+, \cdots, \delta_m^+, \delta_{m+1}^0, \cdots, \delta_l^0) \\ A_c^2 = A(\delta_1^-, \delta_2^+, \cdots, \delta_m^+, \delta_{m+1}^0, \cdots, \delta_l^0) \\ \vdots \\ A_c^M = A(\delta_1^-, \delta_2^-, \cdots, \delta_m^-, \delta_{m+1}^0, \cdots, \delta_l^0) \end{cases}$$

and M matrices of the form

$$\begin{cases} B_c^1 = B(\delta_1^+, \delta_2^+, \cdots, \delta_m^+, \delta_{m+1}^0, \cdots, \delta_l^0) \\ B_c^2 = B(\delta_1^-, \delta_2^+, \cdots, \delta_m^+, \delta_{m+1}^0, \cdots, \delta_l^0) \\ \vdots \\ B_c^M = B(\delta_1^-, \delta_2^-, \cdots, \delta_m^-, \delta_{m+1}^0, \cdots, \delta_l^0) \end{cases}$$

We observe that in our context, the number of critical parameters is very limited (two or three at most) and

therefore the construction of the critical matrices is not a serious computational problem.

Next, we consider a specification property S_1 for Algorithm 1 which depends on the controller gains *K*. The property of satisfying S_1 is verified only for the upper and lower values of the critical parameters. We remark that the algorithm terminates after a number of iterations dictated by the Log-over-log Bound providing a set of gains $\{K^1, K^2,\ldots,K^s\}$.

The starting point of **Algorithm 2** (Fig. 3) is the use of these gains. For each gain $K_{rand} = K^j$, j = 1, 2,…,s, the algorithm is based on randomization of all uncertain parameters (and not only the critical ones) within their given intervals, according to a specified distribution $p(\Delta)$. Given accuracy $\varepsilon \in (0,1)$ and confidence $\eta \in (0,1)$, the Chernoff Bound is used for computing the required sample size for the specification property S_2. The empirical probability of satisfaction is computed.

Algorithm 3 (Fig. 4) is finally utilized. This algorithm has a structure similar to Algorithm 2, but a different specification property S_3 based on flying qualities [13] is introduced. The corresponding empirical probability is computed using the same samples size utilized in Algorithm 2.

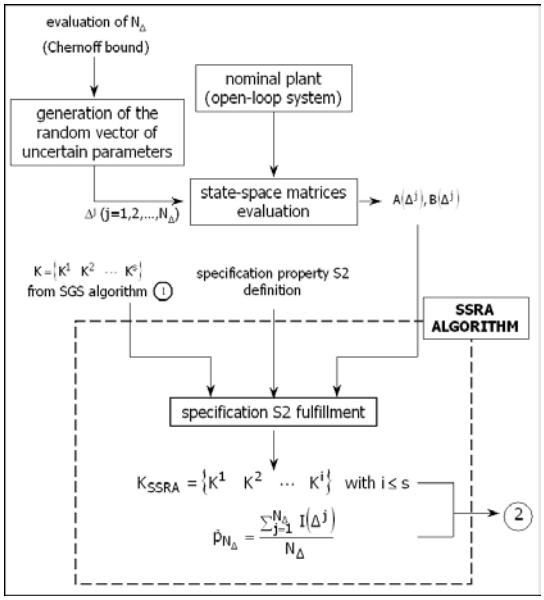

Fig. 3: Algorithm 2 – Probabilistic Robustness Analysis.

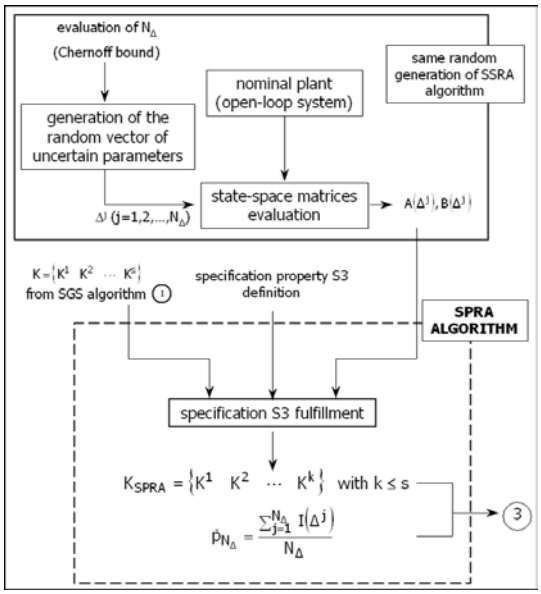

Fig. 4: Algorithm 3 – Probabilistic Robust Performance.

VI NUMERICAL RESULTS

In this section, numerical results are provided. The proposed control design methodology has been applied to the design of an embedded real-time system for autonomous flight control. The autopilot system includes guidance, navigation and loop stabilization. The obtained gain set is used for guidance/trajectory tracking and platform stabilization feedback loops. The guidance laws include altitude/velocity and heading hold loops, while the stabilization issues are related to hold attitude angles and to damp attitude rates by commanding aerodynamic control surface deflections. The proposed gain synthesis methodology can be applied to full state feedback as well as to output feedback control design.

The case study reported here is based on the assumption of decoupled dynamics and it is focused on the longitudinal plane dynamics stabilization. In particular, we restrict our attention to a full state feedback longitudinal control, just demanded to the elevon control surfaces.

The state vector $x \in \mathbf{R}^4$ is defined as:

$$x = [V \quad \alpha \quad q \quad \theta]^T$$

where V is the flight speed, α is the angle of attack, q is the pitch rate and θ is the pitch angle.

The control vector $u \in \mathbf{R}$ is defined as:

$$u = [\delta_e]$$

where δ_e consists of the symmetrical elevon deflection. State and control matrices characterizing the nominal reference condition (V = 13 m/s; h = 50 m) are obtained by numerical linearization:

$$A = \begin{bmatrix} -0.293 & -0.486 & -0.0002 & -9.812 \\ -0.113 & -6.181 & 0.914 & -0.0003 \\ 0.000 & -64.83 & -8.074 & 0.000 \\ 0.000 & 0.000 & 1.000 & 0.000 \end{bmatrix}$$

$$B = \begin{bmatrix} -0.7914 \\ -3.9250 \\ -483.487 \\ 0.000 \end{bmatrix}$$

Next, we observe that structured parameter uncertainties are taken into account, including those related to flight conditions (dynamic pressure), aerodynamic data (stability and control derivatives), geometric and inertial data. Uncertainties related to the flight conditions can be ascribed to the real flight in a non-ideally-calm air and to the need to cover a portion of the flight envelope as large as possible. Uncertainties concerning the aerodynamic data can be related to experimental measurement errors or computational approximations due to numerical evaluation. Finally, uncertainties in terms of geometric and inertial data may take into account manufacturing inaccuracies. Therefore, the vector $\Delta \in \mathbf{R}^{16}$ consisting of uncertain δ_i is described in Table I. For simplicity, only approximate values of upper and lower bounds are shown.

TABLE I. PARAMETER UNCERTAINTIES

Plant and flight condition uncertainties						
#	**parameter**	**p.d.f.**	δ_i	**%**	δ_i^-	δ_i^+
1	flight speed [m/s]	U	13.0	±15	11.0	15.0
2	altitude [m]	U	50.0	±100	0.0	100.0
3	mass [kg]	U	1.5	±10	1.35	1.65
4	wingspan [m]	U	1.0	±5	0.95	1.05
5	mean aero chord [m]	U	0.536	±5	0.509	0.563
6	wing surface [m^2]	U	0.522	±10	0.470	0.574
7	moment of inertia [kgm^2]	U	0.0566	±10	0.0509	0.0623
Aerodynamic database uncertainties						
#	**parameter**	**p.d.f.**	**mean**	**%**	σ_i	
8	C_X coefficient [-]	G	-0.01215	±10	0.0004	
9	C_Z coefficient [-]	G	-0.30651	±5	0.005	
10	C_m coefficient [-]	G	-0.02401	±5	0.0004	
11	C_{Xq} derivative [rad^{-1}]	G	0.20435	±10	0.0065	
12	C_{Zq} derivative [rad^{-1}]	G	-1.49462	±10	0.05	
13	C_{mq} derivative [rad^{-1}]	G	-0.76882	±5	0.01	
14	$C_{X\delta}$ derivative [rad^{-1}]	G	0.17072	±10	0.0054	
15	$C_{Z\delta}$ derivative [rad^{-1}]	G	-1.41136	±5	0.022	
16	$C_{m\delta}$ derivative [rad^{-1}]	G	-0.94853	±5	0.015	

In the remaining of the Section the obtained numerical results characterizing the three phases previously described are presented.

Phase 1: Random Gain Synthesis

As critical uncertain parameters for random gain selection flight speed and mass are chosen, i.e. the vector Δ_c is defined as:

$$\Delta_c = [\delta_1, \delta_3]^T$$

The flight speed has been chosen as critical parameter in order to optimize gain scheduling issues, while the take-off mass represents a key parameter in mission profile definition and flight performance evaluation. The lower and upper bounds of the critical uncertain parameters are reported in Table I.

The specification property S_1 is defined as follows:

$$S_1 = \{K \in \mathcal{B}_K : A_{cl}(K) = A_c\text{-}B_cK \text{ satisfies the properties listed below}\}$$

$$\mathrm{Im}(\lambda_i) \neq 0$$

$$\mathrm{Re}(\lambda_i) < 0$$

$$4.0 \text{ rad/s} < \omega_{SP} < 6.0 \text{ rad/s}$$

$$0.5 < \zeta_{SP} < 0.9$$

$$1.0 \text{ rad/s} < \omega_{PH} < 1.5 \text{ rad/s}$$

$$0.1 < \zeta_{PH} < 0.3$$

$$\Delta\omega_{SP} = \omega_{SP}\big|_{upper} - \omega_{SP}\big|_{lower} < \pm 45\%$$

$$\Delta\omega_{PH} = \omega_{PH}\big|_{upper} - \omega_{PH}\big|_{lower} < \pm 20\%$$

where λ_i represents the eigenvalues and ω and ζ are the undamped natural frequency and damping ratio of the system characteristic modes, respectively. The subscript SP and PH refer to the short period and the phugoid mode, representing the two dynamic modes characterizing the aircraft motion in the longitudinal plane. The specification property definition is strictly related to the user needs in terms of mission profile and to the reference platform. From the properties specified above, it can be observed that a completely decoupled dynamics with classical modal characterization (two periodic stable modes) are required for the MH1000 platform.

The number of random samples for the K matrix, computed according to the Log-over-log Bound with $\varepsilon = 4 \cdot 10^{-5}$ and $\eta = 3 \cdot 10^{-4}$, is $N_K = 200{,}000$. The obtained set of random gains satisfying the specification property S_1 are reported in Table II.

TABLE II. RANDOM GAIN SET FROM GAIN SYNTHESIS

Gain set	K_V	K_α	K_q	K_θ
K1	0.00044023	0.09465	0.015774	-0.0047351
K2	0.00021545	0.095812	0.015555	-0.0032351
K3	0.00054999	0.094308	0.015482	-0.0048634
K4	0.00010855	0.091832	0.01530	-0.0040438
K5	0.00039238	0.094827	0.016093	-0.0041734

Phase 2: Probabilistic Robustness Analysis

The uncertain parameters considered in the case study, their nominal values, probability density function and tolerances are given in Table I. As can be observed from Table I, uniform and gaussian probability density functions have been used to characterize parameter uncertainties: geometric, inertial and operational uncertainties are characterized by uniform p.d.f. while the set of uncertainties related to the aerodynamic database are characterized by a gaussian p.d.f. This criterion has been adopted due to the nature of the parameters: the uncertain

value of the aerodynamic derivative has to be intended with higher probability close to the nominal value experimentally or numerically obtained. Since the aerodynamic data vary as a function of the velocity, the mean value as well as the variance of the uncertainties corresponding to these parameters are approximate values referring to a fixed operating condition.

The specification property S_2 is defined as follows:

$$S_2 = \{\Delta \in \mathcal{B}_\Delta : A_{cl}(\Delta) = A_c(\Delta)\text{-}B_c(\Delta)K_{rand} \text{ satisfies the related properties}\}$$

The user defined properties related to S_2 are the same as for S_1. The number of samples for the specification property S_2, is obtained by the Chernoff bound with $\varepsilon = 0.0145$ and $\eta = 0.0145$, and it is equal to $N_\Delta = 5{,}000$.

The results in terms of estimated probability of stability are reported in Table III.

TABLE III. ESTIMATED PROBABILITY OF STABILITY RELATED TO PHASE 2 (SSRA) AND PHASE 3 (SPRA)

Gain set	SSRA	SPRA
K1	88.56	93.58
K2	90.60	95.16
K3	89.31	90.80
K4	93.86	84.78
K5	85.14	96.06

The estimated probability of stability characterizes the level of matching the desired dynamics and it represents a key feature to choose the "best robust solution". To this end, graphical tools have been also utilized to perform robustness analysis of the designed closed loop system. As an example, Fig. 5 reports the root locus plot for two different solutions, characterized by different probability levels $p_{N\Delta}$. It can be observed that the closed loop system obtained by the random gain set K_2 fulfilling specification property S_1 could give raise to some unstable conditions when all uncertain parameters are considered. Therefore, even if the associated probability of stability is high, it is not considered as a "good" gain and it is consequently discarded.

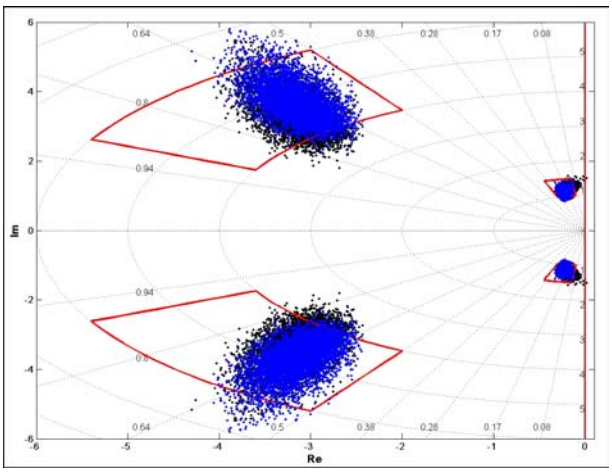

Fig. 5: Root locus plot for K_2 (black) and K_4 (blue) highlighting the regions of interest for stability robustness analysis.

Phase 3: Probabilistic Robust Performance

The uncertain parameters and the random samples N_Δ considered for the Phase 3 of the proposed methodology are the same as for the Phase 2 (Table I).

The specification property S_3 is defined as follows:

$$S_3 = \{\Delta \in \mathcal{B}_\Delta : A_{cl}(\Delta) = A_c(\Delta)\text{-}B_c(\Delta)K_{rand} \text{ satisfies the properties listed below}\}$$

$$2.5 \text{ rad/s} < \omega_{BW} < 5.0 \text{ rad/s}$$

$$0.0 < \tau_P < 0.05$$

where ω_{BW} and τ_P are the bandwidth and the phase delay of the frequency response, respectively. The specification property S_3 is defined accordingly to the bandwidth criterion reported in the aeronautical standards [13]. A graphical approach to the performance robustness analysis, based on the bandwidth criterion plot, has been added to the evaluation of the empirical probability of satisfaction of the specification property. The case study discussed here does not include properties related to time domain response.

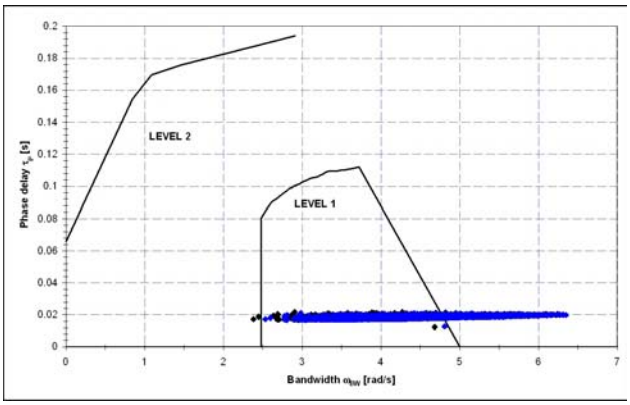

Fig. 6: Bandwidth criterion plot for K_1 (black) and K_3 (blue) highlighting the regions of interest for performance robustness analysis.

The results in terms of estimated probability of stability are reported in Table III. Differences could be shown for the probability values between SSRA and SPRA results: they can be due to the dependence of the stability criteria on the user's experience and knowledge about the plant dynamics despite of the relationships of the performance metrics with the standard requirements. For the present case study, the K_1 solution has been chosen as the best fit solution according to a compromise between the stability and the performance metrics.

VII CONCLUSION AND REMARKS

In this paper, we developed a methodology, based on the theory of randomized algorithms, for gain selection and robustness analysis of the Mini-UAV platform MH1000. The proposed methodology demonstrates to resolve successfully some critical issues arising when classical/modern control techniques are used. In particular, the numerical results given in Section VI enable the aerospace engineer to compute the estimated probability that specific performance requirements are met.

Subsequent research will be performed utilizing different control structures, thus showing the flexibility of the approach in different contexts.

An extended version of this paper has been submitted to an international journal for possible publication.

ACKNOWLEDGMENT

This project is supported by the Italian Ministry for Instruction, University, and Research (MIUR) within the frame of the project PRIN 2004 (Project Number. 2004095094): Study and development of a real-time land control and monitoring system for fire prevention. The aerial platform is based on the MicroHawk configuration, developed at the Aerospace Engineering Dept. of Politecnico di Torino (national patent no. TO2003A000702, holder Politecnico di Torino, international request PCT/IB2004/002940).

REFERENCES

[1] W.R. Davis, "MicroUAVs", 23rd Annual AUVSI Symposium, 1996.

[2] F. Quagliotti, G. Guglieri G., B. Pralio and L. Lorefice, "Simulation Tools for Flight Dynamics Analysis in the Design of MAVs", 24th ICAS Congress, Yokohama, Japan, 2004.

[3] M. Elgersma, S. Gangli, V. Ha and T. Samad, "Statistical Performance Verification for an Autonomous Rotorcraft", Proc. of IEEE International Symposium on Intelligent Control, Taipei, Taiwan, 2004.

[4] K. Zhou and J.C. Doyle and K. Glover, "Robust and Optimal Control", Prentice-Hall, Upper Saddle River, 1996.

[5] R. Tempo, G. Calafiore and F. Dabbene, "Randomized Algorithms for Analysis and Control of Uncertain Systems", Springer-Verlag, London, 2005.

[6] R.F. Stengel, "Some Effects of Parameter Variations on the Lateral-Directional Stability of Aircraft", AIAA Journal of Guidance and Control, Vol. 3, pp. 124-131, 1980.

[7] L.R. Ray and R.F. Stengel, "A Monte Carlo Approach to the Analysis of Control System Robustness", Automatica, Vol. 29, pp. 229-236, 1993.

[8] Q. Wang and R.F. Stengel, "Robust Nonlinear Flight Control of a High Performance Aircraft", IEEE Transactions on Control Systems Technology, Vol. 13, pp. 15-26, 2005.

[9] Q. Wang and R.F. Stengel, "Probabilistic Control of Nonlinear Uncertain Dynamic Systems", in Probabilistic and Randomized Methods for Design under Uncertainty, Springer-Verlag, London, pp. 381-414, 2006.

[10] B.L. Stevens and F.L. Lewis, "Aircraft Control and Simulation", John Wiley & Sons Inc., 2003.

[11] R. Tempo, E.W. Bai and F. Dabbene, "Probabilistic Robustness Analysis: Explicit Bounds for the Minimum Number of Samples",' Systems and Control Letters, Vol. 30, pp. 237-242, 1997.

[12] H. Chernoff, "A Measure of Asymptotic Efficiency for Tests of a Hypothesis Based on the Sum of Observations", Annals of Mathematical Statistics, Vol. 23, pp. 493-507, 1952.

[13] Anonymous, "Flying Qualities of Piloted Aircraft", MIL-HDBK-1797, Department of Defense, USA, 1997.

[14] B. McCormick, "Aerodynamics, aeronautics and flight mechanics", John Wiley & Sons Inc., 1995.